

FREE VIBRATION OF PIEZOELECTRIC FGM SANDWICH BEAM WITH POROUS CORE EMBEDDED IN THERMAL ENVIRONMENT AND ELASTIC FOUNDATION

Tran Quang Hung^a, Tran Minh Tu^b, Do Minh Duc^{a,*}

^a*Faculty of Civil Engineering, University of Science and Technology, The University of Danang,
54 Nguyen Luong Bang street, Lien Chieu district, Danang City, Vietnam*

^b*Faculty of Building and Industrial Construction, Hanoi University of Civil Engineering,
55 Giai Phong road, Hai Ba Trung district, Hanoi, Vietnam*

Article history:

Received 04/08/2021, Revised 07/09/2021, Accepted 16/09/2021

Abstract

This paper aims to present thermo-electrical free vibration characteristics of functionally graded material (FGM) sandwich beam placed on the two-parameter elastic foundation. The beam is constructed of a foam core, two middle FGM layers, and two outer piezoelectric layers. It is assumed that the beam is subjected to a constant voltage and a uniform/linear temperature distribution. Physical properties of the core and two middle layers vary smoothly through the thickness according to the cosine and power-law forms, respectively. Lagrange equations in conjunction with the Reddy third-order beam theory is employed to derive the governing equations of motion. A simple polynomial trial function-based Ritz method is adopted for the approximation of the displacement field to obtain the vibration response. The correctness of the study is verified by comparisons with other authors' published results. Influences of geometry parameters, material property distribution, applied voltage, elastic foundation, temperature distribution, temperature change, porosity coefficient, span-to-height ratio, and boundary conditions are investigated through parametric studies.

Keywords: thermo-electrical vibration; porous sandwich beam; functionally graded material; thermo-piezoelectricity; Ritz method; two-parameter foundation.

[https://doi.org/10.31814/stce.huce\(nuce\)2021-15\(4\)-02](https://doi.org/10.31814/stce.huce(nuce)2021-15(4)-02) © 2021 Hanoi University of Civil Engineering (HUCE)

1. Introduction

Sandwich beams consisting of two outer layers and a porous core is a form of the lightweight beam structure. While the face layers are thin but strong to carry the bending and in-plane loads, the thick porous core connects the face layers, sustains the shear force and minimizes the self-weight. Besides, the porous core with porosities inside enhances good functions, such as sound absorption, thermal insulation, energy dissipation, etc.

Over the past few years, the mechanical behavior of this beam type has been investigated by using many beam models and computational methods. The Euler-Bernoulli beam theory that neglecting transverse shear deformation is the most simple model commonly used for preliminary design purposes. For the thicker beams, the Timoshenko beam model known as first-order beam theory (FOBT) is an appropriate choice, but the shear correction factor must be included. To overcome this difficulty,

*Corresponding author. *E-mail address:* ducdbk@gmail.com (Duc, D. M.)

higher-order beam theories (HOBTs) are proposed. The sandwich beam composed of a porous core and isotropic face sheets have been used as lightweight structures in many areas and extensively studied. Chen et al. [1] investigated the nonlinear free vibration of sandwich Timoshenko porous beams by employing the Ritz method. The free vibration analysis of porous sandwich beams having metal foam core and interacting with Winkler–Pasternak foundation was conducted by Wang and Zhao [2] using the Chebyshev collocation method and the FOBT. Grygorowicz et al. [3] dealt with the elastic buckling of a porous sandwich beam with a metal foam core by both analytical and numerical methods. Srikarun et al. [4] studied the linear and nonlinear bending of sandwich beams with foam cores under different kinds of distributed load utilizing the GramSchmidt-Ritz procedure together with the third-order beam theory (TOBT).

The sandwich beam with face sheets made of functionally graded materials (FGMs) is the choice for the beams that working in higher temperature environments. Obviously, the porous sandwich beam with FG face sheets is an advanced lightweight structure and has multi-advantages for applications. Therefore, studying to comprehend the mechanical behavior of this beam has received attention from engineers and scientists. Wang et al. [5] studied the time history response of the beam subjected to a non-uniformly distributed moving mass based on the HOBT and Chebyshev–Ritz technique. Hung and Truong [6] examined analytically the natural frequencies of the beam resting on the Winkler foundation using different beam theories. Developing a 1D mesh-free method in conjunction with TOBT, Chinh et al. [7] investigated the static bending of the beam under distributed loads. Mu and Zhao [8] dealt with the first frequency of the beam by the extended Galerkin method. Derikvand and coworkers [9] presented the buckling characteristics of the beam with a porous ceramic core using the differential transform method, TOBT, and a two-variable refined shear deformation theory.

Piezoelectric materials are known as smart materials which are often integrated into structures to control and/or monitor their response. To combine the advantages of piezoelectric materials and FGMs, FGM beams integrated with piezoelectric layers have been proposed, and their mechanical response should be analyzed. Several studies on FGM beams bonded with the piezoelectric layers have been performed and reported in the open literature. Based on the closed-form solutions, Kiani et al. [10] studied the thermal buckling of Timoshenko beams with/without surface-bonded piezoelectric layers under both thermal and electrical loadings. Kargani et al. [11] presented an exact solution for the post-buckling of piezoelectric FGM Timoshenko beams subjected to coupled thermo-electrical loadings. She et al. [12] investigated the thermal buckling and post-buckling of FGM beams with/without piezoelectric outer layers using HOBT and a two-step perturbation method. Fu et al. [13] dealt with the thermal buckling, nonlinear free vibration, and dynamic stability of piezoelectric FGM beam by analytical solution, the classical beam theory and the physical neutral concept. Khiem et al. [14] investigated the effects of a piezoelectric patch bonded to FGM Timoshenko beams on the free vibration of the beams by the dynamic stiffness method. Jankowski et al. [15] focused on the mechanical and electrical buckling of piezoelectric FGM porous nanobeams based on a higher-order nonlocal elasticity and strain gradient theory. In this work, the analytical solution in conjunction with Reddy's beam theory was used. Singh and Kumari [16] presented an analytical solution based on piezoelectricity for two-dimensional free vibration analysis of axially FGM beam integrated with piezoelectric layers.

In order to more accurately predict the static and dynamic response of sandwich beams, finding appropriate beam models and computational tools is always motivation for the researches of the scientist. Other than the above-mentioned theories, Reddy third-order beam theory (ROBT) is used in many published reports [4, 15, 17, 18]. This theory belongs to HOBTs, and accounts for the parabolic distribution of the transverse shear strains through the height of the beam and satisfies zero shear

stresses conditions on the surfaces of the beam. Although it is not as accurate as the 3D or quasi-3D beam theories in reflecting the working of all types of beams, the ROBT is still the preferred choice due to having the same dependent unknowns as in FOBT without using the shear correction factor.

There are many numerical methods commonly used to solve mechanical problems such as finite element method, shooting method, mesh-free method, Ritz method, differential transform method, Galerkin method, Chebyshev collocation method, etc. Among them, the Ritz method is a variational method that is based on seeking an approximate solution in the form of a linear combination of suitable approximation functions and undetermined parameters [19]. In spite of some limitations, such as it is possible only if a suitable function is available, the number of terms is a key factor in deciding the convergence, the accuracy, and stability of the solution are dependent on the accuracy of shape function, etc. [20], Ritz method could be efficiently applied for simple configurations, such as single-span beams, rectangular/circular plates, etc. It can also be an alternative selection for mechanical problems with general boundary conditions when Navier’s method is limited.

The literature review reveals that there has not been any study on sandwich beams with metal foam core subjected to simultaneous effects of mechanical, electrical and thermal loading. Thus, in this paper, thermo-electrical free vibration frequencies of FGM sandwich beams resting on Pasternak foundation are investigated. The beam has layer structure as a foam core, two middle FGM layers, and two outer piezoelectric layers. Physical properties of the core and two FGM layers vary smoothly across the thickness according to the cosine and power-law forms, respectively. The beam is pre-stressed through a constant voltage and a uniform/linear temperature rise. Based on ROBT as well as Lagrange equations, the governing equations of motion are derived. A simple polynomial trial function-based Ritz method is adopted to obtain the approximate solution. The accuracy of the study is verified by comparisons with other authors’ published results through numerical examples. Influences of geometry parameters, material property distribution, applied voltage, elastic foundation, temperature rises, temperature change, porosity coefficient, span-to-height ratio, and boundary conditions on the vibration frequencies are examined and discussed.

2. Theory and basic equations

2.1. Geometrical parameters and layer structure of piezoelectric FGM sandwich beam

Consider a piezoelectric FGM sandwich beam of length L , cross-section $b \times h$, and symmetric layer structure as shown in Fig. 1. The thickness is $h = 2h_a + 2h_f + h_c$. The beam places on the two-parameter Pasternak foundation, and the x -axis coincides with the geometrical mid-surface.

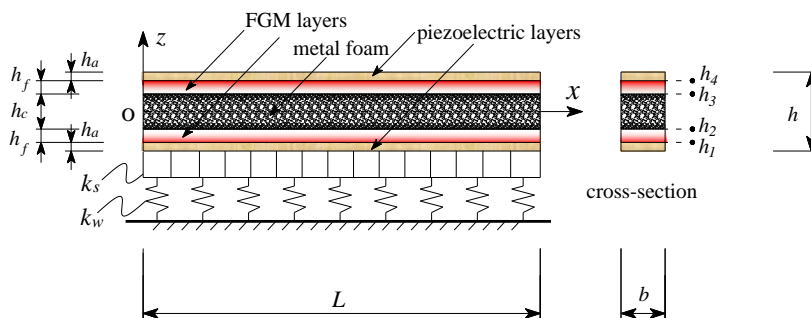


Figure 1. Geometry of piezoelectric FGM sandwich beam on elastic foundation

2.2. Physical property distribution

The two piezoelectric layers are made of a homogeneous and isotropic material. The foam core and two FGM layers, respectively, have physical properties varied continuously according to the cosine and power-law forms as follows.

$$\begin{cases} O(z) = (O_m - O_c) [(h_4 - z) / (h_4 - h_3)]^k + O_c, & h_3 \leq z \leq h_4 \\ O(z) = O_m [1 - e_o \cos(\pi z / (h_3 - h_2))], & h_2 \leq z \leq h_3 \\ O(z) = (O_m - O_c) [(z - h_1) / (h_2 - h_1)]^k + O_c, & h_1 \leq z \leq h_2 \end{cases} \quad (1)$$

$$\begin{cases} \rho(z) = (\rho_m - \rho_c) [(h_4 - z) / (h_4 - h_3)]^k + \rho_c, & h_3 \leq z \leq h_4 \\ \rho(z) = \rho_m [1 - e_m \cos(\pi z / (h_3 - h_2))], & h_2 \leq z \leq h_3 \\ \rho(z) = (\rho_m - \rho_c) [(z - h_1) / (h_2 - h_1)]^k + \rho_c, & h_1 \leq z \leq h_2 \end{cases} \quad (2)$$

In Eqs. (1) and (2), O stands for elastic modulus E , thermal expansion coefficient α ; k is the power-law index; ρ is the mass density; e_o is the porosity coefficient; the porosity coefficient for mass density e_m is determined by the relation $e_m = 1 - \sqrt{1 - e_o}$ [1]. The subscripts “ c ” and “ m ” denote the ceramic and metal materials which constitute the beam. The Poisson’s ratio ν is summed to be unchanged in each layer.

2.3. Temperature distributions

In this study, two typical types of temperature distribution along the beam thickness, i.e., uniform temperature rise (UTR) and linear temperature rise (LTR), are supposed. The beam is assumed to have no thermal stresses at the temperature $T_0 = 300$ K.

a. Uniform temperature rise

The whole domain of the beam is subjected to a temperature change Δt from the initial temperature T_0 . Hence, the current temperature $T(z)$ at any point in the beam can be written as

$$T(z) = T_0 + \Delta T \quad (3)$$

b. Linear temperature rise

The temperature field in the beam varies linearly along the thickness and could be expressed as

$$T(z) = t_L + \Delta T (z/h + 1/2); \quad \Delta T = (t_U - t_L) \quad (4)$$

where t_U and t_L are current temperatures at the bottom ($z = -h/2$) and the top ($z = h/2$) of the beam, respectively. Unless otherwise stated, $t_L = T_0 = 300$ K throughout the study.

2.4. Displacement and strain fields

In this study, ROBT [17, 18] is employed. The displacement components u, w , respectively, in x - and z -directions can be expressed:

$$\mathbf{d} = \begin{Bmatrix} u \\ w \end{Bmatrix} = \begin{bmatrix} 1 & 0 & -z & f(z) \\ 0 & 1 & 0 & 0 \end{bmatrix} \mathbf{A}_1 \quad (5)$$

$$\mathbf{A}_1^T = \left\{ u_o(x, t) \quad w_o(x, t) \quad \frac{\partial w_o(x, t)}{\partial x} \quad \phi_{os}(x, t) \right\}; \quad f(z) = z \left(1 - \frac{4z^2}{3h^2} \right) \quad (6)$$

where u_o, w_o, ϕ_{os} are three unknown displacements on the mid-surface of the beam. The strain tensor can be determined by taking the derivatives of the displacements and described as

$$\boldsymbol{\varepsilon} = \begin{Bmatrix} \varepsilon_x \\ \gamma_{xz} \end{Bmatrix} = \begin{bmatrix} 1 & -z & f(z) & 0 \\ 0 & 0 & 0 & \frac{\partial f(z)}{\partial z} \end{bmatrix} \mathbf{A}_2 \quad (7)$$

$$\mathbf{A}_2^T = \begin{Bmatrix} \frac{\partial u_o}{\partial x} & \frac{\partial^2 w_o}{\partial x^2} & \frac{\partial \phi_{os}}{\partial x} & \phi_{os} \end{Bmatrix} \quad (8)$$

2.5. Constitutive relation

For the foam core and two middle FGM layers, ($h_1 \leq z \leq h_4$), based on Hook's law, the constitutive equations including the thermal effect can be written below

$$\begin{cases} \sigma_x = E [\varepsilon_x - \alpha(T - T_0)]; & \tau_{xz} = G\gamma_{xz} \\ G = E / (2 + 2\nu) \end{cases} \quad (9)$$

In the case of the piezoelectric layers, ($h_1 - h_a \leq z \leq h_1$) \cup ($h_4 \leq z \leq h_4 + h_a$), the constitutive equations including both the thermal and electrical effects may be written as follows [11]

$$\begin{cases} \sigma_x = E_a \{ \varepsilon_x - \alpha_a(T - T_0) - d_{31}E_z \}; & \tau_{zx} = G_a\gamma_{xz} \\ E_z = V_o/h_a; & G_a = E_a / (2 + 2\nu_a) \end{cases} \quad (10)$$

In Eqs. (9) and (10), σ_x, σ_{xz} are the axial and shear stresses, respectively; V_o is the applied voltage across the thickness of the piezoelectric layers; d_{31} is the dielectric permittivity coefficient [10–12]. The subscript “a” denotes the properties that belong to the piezoelectric material.

2.6. Energy expressions and governing equations

Internal strain energy due to the mechanical stresses, neglecting thermo-electrical effects, can be calculated by following formulations

$$U^m = \frac{1}{2} \int_V \begin{Bmatrix} \sigma_x \\ \tau_{xz} \end{Bmatrix}^T \boldsymbol{\varepsilon} dV = \frac{1}{2} \int_V \boldsymbol{\varepsilon}^T \mathbf{E}_d \boldsymbol{\varepsilon} dV = \frac{1}{2} \int_0^L \mathbf{A}_2^T \mathbf{D}_E \mathbf{A}_2 dx \quad (11)$$

where

$$\mathbf{E}_d = \begin{bmatrix} E, E_a & 0 \\ 0 & G, G_a \end{bmatrix} \quad (12)$$

$$\mathbf{D}_E = b \int_{-h/2}^{h/2} \begin{bmatrix} 1 & -z & f(z) & 0 \\ 0 & 0 & 0 & \frac{\partial f(z)}{\partial z} \end{bmatrix}^T \mathbf{E}_d \begin{bmatrix} 1 & -z & f(z) & 0 \\ 0 & 0 & 0 & \frac{\partial f(z)}{\partial z} \end{bmatrix} dz \quad (13)$$

In Eq. (12) E and G are used when formulating for the core and FGM layers, whereas E_a and G_a are for the piezoelectric layers

The potential energy of the elastic foundation can be expressed as

$$U^f = \frac{1}{2} b \int_0^L \left\{ k_w w_o^2 + k_s \left(\frac{\partial w_o}{\partial x} \right)^2 \right\} dx = \frac{1}{2} b \int_0^L \left\{ k_w w_o^2 + k_s \left(\frac{\partial w_o}{\partial x} \right)^2 \right\} dx \quad (14)$$

where k_w and k_s are the two elastic coefficients of the Pasternak foundation.

The work done by thermal and electrical stress resultants is written as

$$V = \frac{1}{2} \int_0^L N^e \left(\frac{\partial w_o}{\partial x} \right)^2 dx + \frac{1}{2} \int_0^L N^{th} \left(\frac{\partial w_o}{\partial x} \right)^2 dx \quad (15)$$

where N^e is the electrical stress resultant of the outer piezoelectric layers, and N^{th} is the thermal stress resultant. They are defined as

$$\begin{cases} N^e = -2bV_oE_a d_{31} \\ N^{th} = -b \int_{h_1-h_a}^{h_1} E_a \alpha_a (T - T_0) dz - b \int_{h_1}^{h_4} E \alpha (T - T_0) dz - b \int_{h_4}^{h_4+h_a} E_a \alpha_a (T - T_0) dz \end{cases} \quad (16)$$

The kinetic energy of the beam is presented as

$$K = \frac{1}{2} b \int_0^L \int_{h_1-h_a}^{h_4+h_a} \rho(z) \left[\left(\frac{\partial u}{\partial t} \right)^2 + \left(\frac{\partial w}{\partial t} \right)^2 \right] dx dz = \frac{1}{2} \int_0^L \frac{\partial \mathbf{A}_1^T}{\partial t} \mathbf{D}_R \frac{\partial \mathbf{A}_1}{\partial t} dx \quad (17)$$

where

$$\mathbf{D}_R = b \int_{h_1-h_a}^{h_4+h_a} \rho(z) \begin{bmatrix} 1 & 0 & -z & f(z) \\ 0 & 1 & 0 & 0 \end{bmatrix}^T \begin{bmatrix} 1 & 0 & -z & f(z) \\ 0 & 1 & 0 & 0 \end{bmatrix} dz \quad (18)$$

In this study, Lagrange equations are adopted to derive the equations of motion. These equations are then discretized by Ritz method for the approximate solution.

According to the concept of Ritz method, the displacement functions u_o , w_o , and ϕ_{os} are approximated by series of admissible functions that should satisfy the kinetic boundary conditions. If the functions violate this requirement, additional techniques, such as Lagrange multipliers [21], penalty method [22], can be used to treat; this approach, however, needs more computational effort. Some functions, such as trigonometric, algebraic polynomial, and orthogonal polynomial functions, are often used. In this study, the admissible functions which have polynomial form [23, 24] for single-span beam are selected and given in Table 1. These functions are simple to satisfy different cases of the

Table 1. Polynomial admissible functions with different BCs

BCs	$u_o(x, t)$	$w_o(x, t)$	$\phi_{os}(x, t)$
SS	$\sum_{i=1}^N U_{oi}(t) x^1 (L-x)^1 x^{i-1}$	$\sum_{i=1}^N W_{oi}(t) x^1 (L-x)^1 x^{i-1}$	$\sum_{i=1}^N \Phi_{osi}(t) x^0 (L-x)^0 x^{i-1}$
CH	$\sum_{i=1}^N U_{oi}(t) x^1 (L-x)^1 x^{i-1}$	$\sum_{i=1}^N W_{oi}(t) x^2 (L-x)^1 x^{i-1}$	$\sum_{i=1}^N \Phi_{osi}(t) x^1 (L-x)^0 x^{i-1}$
CC	$\sum_{i=1}^N U_{oi}(t) x^1 (L-x)^1 x^{i-1}$	$\sum_{i=1}^N W_{oi}(t) x^2 (L-x)^2 x^{i-1}$	$\sum_{i=1}^N \Phi_{osi}(t) x^1 (L-x)^1 x^{i-1}$

boundary conditions (BCs) as well as effective in analytical calculations. Different immovable BCs, such as simply-supported (SS), clamped-hinged (CH), and clamped-clamped (CC), are considered.

In Table 1, N is the number of polynomial terms. It is determined in the analysis so that the obtained results satisfy the accuracy. U_{oi} , W_{oi} , Φ_{osi} are the time-dependent unknown coefficients.

Substituting the trial functions in Table 1 into the energy expressions of Eqs. (11), (14), (15) and (17) then applying the Lagrange equations, Eq. (19) below, yields the equilibrium equation system.

$$\begin{cases} \frac{\partial J}{\partial U_{oi}} - \frac{d}{dt} \frac{\partial J}{\partial \dot{U}_{oi}} = 0 \\ \frac{\partial J}{\partial W_{oi}} - \frac{d}{dt} \frac{\partial J}{\partial \dot{W}_{oi}} = 0 \\ \frac{\partial J}{\partial \Phi_{osi}} - \frac{d}{dt} \frac{\partial J}{\partial \dot{\Phi}_{osi}} = 0, \quad i = 1, \dots, N \end{cases} \quad (19)$$

where $J = U^{in} + U^f + V - K$, and the over dot ($\dot{\bullet}$) implies the derivative with respect to time.

Carrying out Eq. (19) leads to a system of linear equations which can be described by a matrix equation as

$$([\mathbf{K}]_{3N \times 3N} + (N^e + N^{th})[\mathbf{K}_G]_{3N \times 3N}) \begin{Bmatrix} \mathbf{U}_o \\ \mathbf{W}_o \\ \Phi_{os} \end{Bmatrix}_{3N \times 1} + [\mathbf{M}]_{3N \times 3N} \begin{Bmatrix} \ddot{\mathbf{U}}_o \\ \ddot{\mathbf{W}}_o \\ \ddot{\Phi}_{os} \end{Bmatrix}_{3N \times 1} = \{0\}_{3N \times 1} \quad (20)$$

where \mathbf{K} , \mathbf{K}_G and \mathbf{M} are the elastic stiffness, geometric stiffness, and mass matrices, respectively.

For free vibration analysis, the displacement functions are harmonic. The time-dependent unknown coefficients could be assumed as sinusoidal form:

$$\begin{Bmatrix} \mathbf{U}_o \\ \mathbf{W}_o \\ \Phi_{os} \end{Bmatrix} = \begin{Bmatrix} \bar{\mathbf{U}}_o \\ \bar{\mathbf{W}}_o \\ \bar{\Phi}_{os} \end{Bmatrix} \sin(\omega t) \quad (21)$$

in which ω is the natural frequency, and $\bar{\mathbf{U}}_o$, $\bar{\mathbf{W}}_o$, $\bar{\Phi}_{os}$ are the vectors of the coefficients of vibration amplitude.

Substituting Eq. (21) back into Eq. (20) leads to the frequency equation as follows

$$([\mathbf{K}]_{3N \times 3N} + (N^e + N^{th})[\mathbf{K}_G]_{3N \times 3N} - \omega^2[\mathbf{M}]_{3N \times 3N}) \begin{Bmatrix} \mathbf{U}_o \\ \mathbf{W}_o \\ \Phi_{os} \end{Bmatrix}_{3N \times 1} = \{0\}_{3N \times 1} \quad (22)$$

For each pair of N^e and N^{th} by the applied thermal and electrical loadings, the non-trivial solution of Eq. (22) yields the natural frequencies ω and their eigenvector that is used to determine the corresponding mode shape. Obviously, by actively adjusting the pre-stress resultant N^e through the electrical voltage V_o , the frequencies can be enhanced.

3. Computational results

In this section, numerical analysis is conducted to validate the developed theories and examine the vibration characteristics of the beam. In the presentation, non-dimensional frequency is defined as [25, 26].

$$\lambda = \frac{\omega L^2}{h} \sqrt{\frac{\rho_m}{E_m}} \quad (23)$$

Also, non-dimensional coefficients of elastic foundation coefficients are introduced by [25].

$$K_w = \frac{12k_w L^4}{E_m b h^3}; \quad K_s = \frac{12k_s L^2}{\pi^2 E_m b h^3} \quad (24)$$

3.1. Validation

For the first validation, consider a single-layer FGM beam by omitting two piezoelectric layers (setting $h_a = 0$), the bottom FGM and the core layers (setting $h_1 = h_2 = h_3 = -h/2$). The beam interacts with the foundation but is not subjected to temperature change ($\Delta T = 0$). Free vibration of this beam was analyzed by Zahedinejad [25]. Mechanical properties of materials and conditions for the analysis are taken the same as Ref. [25]. To be consistent with the study of Zahedinejad [25], interchanging the roles of ceramic (O_c, ρ_c) and metal (O_m, ρ_m), and replacing the minus sign by the plus sign for z variable in Eqs. (1) and (2). The calculated results for some situations are given in Table 2.

Table 2. The first non-dimensional frequency λ_1 of single-layer FGM (Al/Al₂O₃) beam ($L/h = 10, K_w = 10, K_s = 1$)

BCs	Source	Theory	k				
			0	1	2	5	10
SS	Present	ROBT	5.9285	5.1957	5.0418	4.8744	4.6925
	Zahedinejad [25]	HOBT	5.9280	5.1950	5.0410	4.8740	4.6920
CC	Present	ROBT	11.9739	9.5200	8.7706	8.3047	8.0573
	Zahedinejad [25]	HOBT	11.9690	9.5170	8.7680	8.3020	8.0540

The second validation is devoted to a solid FGM sandwich beam without piezoelectric layers, thermal environment, and foundation by setting $h_a = 0, k_w = k_s = 0, e_o = 0$, and $\Delta T = 0$ in the analysis. The natural frequencies of this beam type were studied by Vo et al. [26]. The same materials and working conditions as Ref. [26] are applied for the analysis. Some obtained results are listed in Table 3.

Table 3. The first non-dimensional frequency λ_1 of FGM (Al/Al₂O₃) sandwich beam with soft core ($L/h = 5, h_c/h_f = 8$)

BCs	Source	Theory	k					
			0	0.5	1	2	5	10
SS	Present	ROBT	2.6773	3.4342	3.7064	3.9303	4.1139	4.1855
	Ref. [26]	HOBT	2.6773	3.4342	3.7065	3.9303	4.1139	4.1855
CC	Present	ROBT	5.2330	6.3348	6.6721	6.9250	7.1173	7.1903
	Ref. [26]	HOBT	5.2311	6.3333	6.6705	6.9233	7.1155	7.1884

The third validation is performed for the case of piezoelectric FGM beam without thermal environment and foundation by setting $h_1 = h_2 = h_3 = -h/2 + h_a, k_w = k_s = 0$, and $\Delta T = 0$ in the analysis. Vibration problems of this beam type with CC end supports were dealt by Fu et al. [13]. FGM is composed of Silicon nitride (Si₃N₄) and stainless steel (SUS304), and the geometry parameters are

taken as $L = 200$ mm, $h = 10$ mm, and $h_a = 1$ mm (Fu et al. [13]). In order to be consistent with the study of Fu et al. [13] in which Euler beam theory was employed, the unknown component is set to zero in the analysis. Also, Eqs. (1) and (2) describing physical properties of FGM layer $\phi_{os}(x, t)$ is treated the same as the first validation. The first non-dimensional frequency is reported and compared with those of Fu et al. [13] as in Table 4.

Table 4. The first non-dimensional frequency $\lambda_1 = \omega_1 L \sqrt{\rho_c/E_c}$ of piezoelectric single-layer FGM ($\text{Si}_3\text{N}_4/\text{SUS304}$) beam

Source	V_o (V)	k				
		0	0.5	1	2	5
Present	200	0.21826	0.17012	0.15440	0.14229	0.13209
Fu et al. [13]	200	0.22264	0.17358	0.15753	0.14516	0.13473
Present	-200	0.21834	0.17019	0.15447	0.14236	0.13215
Fu et al. [13]	-200	0.22273	0.17366	0.15760	0.14523	0.13480

Further validation is conducted for free vibration of single-layer porous beam without thermal environment and foundation by setting $h_a = 0, h_1 = h_2 = -h/2, h_3 = h_4 = h/2, k_w = k_s = 0$, and $\Delta T = 0$. The material properties of the porous beam are $E_m = 200$ GPa, $\rho_m = 7850$ kg/m³, $\nu_m = 0.33$ and $e_o = 0.5$ [27]. Some values of the first non-dimensional frequency are reported and compared with the previous publish of Noori et al. [27] in Table 5.

Table 5. The first non-dimensional frequency λ_1 of single-layer porous beam

BCs	$L/h = 20$		$L/h = 50$	
	Present (ROBT)	Ref. [27] (FOBT)	Present (ROBT)	Ref. [27] (FOBT)
CC	6.3366	6.3476	6.4569	6.4588
CH	4.4080	4.4125	4.4566	4.4574

Table 6. The first non-dimensional frequency $\lambda_1 = \frac{\omega_1 L^2}{h} \sqrt{I_o/E_o}$ of single-layer FGM ($\text{Al}_2\text{O}_3/\text{SUS304}$) beams

$$\text{under UTR } (L/h = 30, I_o = \int_{-h/2}^{h/2} \rho_m dz, E_o = \int_{-h/2}^{h/2} E_m dz)$$

BCs	Source	Theory	$k = 0.2$			$k = 2$		
			$\Delta T = 0$ K	50 K	100 K	$\Delta T = 0$ K	50 K	100 K
CC	Present	ROBT	6.6377	6.1201	5.5493	6.7344	5.9824	5.1091
	Ref. [28]	HOBT	6.6373	6.1198	5.5490	6.7339	5.9821	5.1090
CH	Present	ROBT	4.5902	3.8552	2.9280	4.6625	3.5699	1.8882
	Ref. [28]	HOBT	4.5901	3.8552	2.9281	4.6625	3.5699	1.8886

Final validation is carried out for thermal vibration of a single-layer FGM ($\text{Al}_2\text{O}_3/\text{SUS304}$) beam without an elastic foundation. To reduce to the single-layer FGM beam, the conditions for layer structure in the analysis are set the same as the first validation. The material properties, as well as the relationship between stresses and strains, are chosen as the study by Nguyen et al. [28] for the verification purpose. The first non-dimensional frequencies of the beam under UTR are presented in

Table 6. Observing all the data from comparative studies in Tables 2–6 can conclude that the correctness of the current study is excellently achieved.

3.2. Comprehensive studies

In the next examples, materials which compose the beam are taken from the papers of Kiani et al. [10], She et al. [12], Fu et al. [13], and Vo et al. [26]. Metal is Aluminum (Al): $E_m = 70$ GPa, $\rho_m = 2702$ kg/m³, $\alpha_m = 23 \times 10^{-6}$ /K. Ceramic is Alumina (Al₂O₃): $E_c = 380$ GPa, $\rho_c = 3960$ kg/m³, $\alpha_c = 7.4 \times 10^{-6}$ /K. PZT-5A is selected for the piezoelectric layers. Its properties are $E_a = 63$ GPa, $\rho_a = 7600$ kg/m³, $d_{31} = 2.54 \times 10^{-10}$ m/V, $\alpha_a = 0.9 \times 10^{-6}$ /K. Poisson’s ratio in the whole domain is assumed to be constant ($\nu = \nu_a = 0.3$). Geometrical parameters of the cross-section are $h = 0.06$ m, $h_f = 0.005$ m, $h_c = 0.04$ m, $h_a = 0.005$ m; the width of the beam is unity.

Table 7 presents the first non-dimensional frequency λ_1 of the piezoelectric sandwich beam calculated for different values of applied voltage and temperature change. It is seen that increasing the applied voltage and/or temperature change leads to the decrease of λ_1 . This is because the compressive pre-stress resultant ($N^e + N^{th}$) increases as V_o and/or ΔT increases which reduces the stiffness of the system. It is also pointed out that the applied voltage in the piezoelectric layers has little effect, whereas temperature change has a strong effect on the frequency. Besides, under the same temperature change ΔT , UTR, with all points in the cross-section of the beam subjected to the same ΔT , gives much lower values of λ_1 than LTR does. In addition, it is interesting that the frequency predicted by UTR and $\Delta T = 40$ K is identical to that predicted by LTR and $\Delta T = 80$ K for the same situation of V_o . In general, the reason is the symmetry of the layer structure; hence, the thermal pre-stress resultant N^{th} caused by UTR with ΔT is equal to that caused by LTR with $2 \times \Delta T$.

Table 7. The first non-dimensional frequency λ_1 of the piezoelectric FGM sandwich porous beam (SS, $K_w = 10, K_s = 0.5, L/h = 20, e_o = 0.6$)

Temperature rise	V_o (V)	$\Delta T = 0$ K		$\Delta T = 40$ K		$\Delta T = 80$ K	
		$k = 0.5$	$k = 5$	$k = 0.5$	$k = 5$	$k = 0.5$	$k = 5$
UTR	500	3.6519	4.1191	3.4000	3.8984	3.1280	3.6645
	200	3.6529	4.1200	3.4011	3.8994	3.1292	3.6655
	0	3.6536	4.1206	3.4019	3.9000	3.1300	3.6662
	-200	3.6543	4.1212	3.4026	3.9006	3.1308	3.6669
	-500	3.6554	4.1221	3.4038	3.9016	3.1320	3.6679
LTR	500	3.6519	4.1191	3.5282	4.0103	3.4000	3.8984
	200	3.6529	4.1200	3.5293	4.0112	3.4011	3.8994
	0	3.6536	4.1206	3.5300	4.0118	3.4019	3.9000
	-200	3.6543	4.1212	3.5307	4.0124	3.4026	3.9006
	-500	3.6554	4.1221	3.5318	4.0134	3.4038	3.9016

Table 8 reports the first non-dimensional frequency λ_1 for different values of elastic foundation coefficients (K_w, K_s) and of the power-law index k . The obtained results show that λ_1 increases when the power-law index and/or foundation coefficients increases. The reason is that increasing in the value of those parameters makes the system become stiffer.

Fig. 2 plots the variation of the lowest non-dimensional frequency λ_1 versus the porosity coefficient e_o for two cases of temperature rise, i.e., UTR and LTR. It is seen that the frequency increases with the increase of e_o for all cases of the temperature change, even if $\Delta T = 0$. The greater ΔT is, the greater the rate of the increase in λ_1 with respect to e_o is. This confirms the effectiveness of porosity

Table 8. The first non-dimensional frequency λ_1 of the piezoelectric FGM sandwich porous beam (CC, $L/h = 30, e_o = 0.6, V_o = 200 \text{ V}, \Delta T = 60 \text{ K}$)

UTR/LTR	K_w	K_s	k						
			0	0.2	0.5	1	2	5	10
UTR	0	0	5.0807	5.6932	6.2545	6.7623	7.2171	7.6183	7.7820
	10	0.0	5.1517	5.7559	6.3110	6.8140	7.2651	7.6633	7.8259
	10	0.5	5.5631	6.1225	6.6430	7.1189	7.5484	7.9293	8.0852
	102	0.5	6.1222	6.6291	7.1076	7.5497	7.9516	8.3101	8.4572
	102	1.0	6.4696	6.9479	7.4024	7.8247	8.2103	8.5551	8.6969
LTR	0	0	5.3677	5.9918	6.5462	7.0391	7.4758	7.8577	8.0127
	10	0.0	5.4349	6.0514	6.6002	7.0888	7.5221	7.9013	8.0553
	10	0.5	5.8244	6.3994	6.9169	7.3812	7.7951	8.1587	8.3067
	102	0.5	6.3605	6.8857	7.3643	7.7975	8.1862	8.5293	8.6692
	102	1.0	6.6940	7.1916	7.6480	8.0630	8.4367	8.7674	8.9025

in increasing the frequency of porous structures, especially when the structures work in a high temperature environment. Also, as discussed about the predicted results in Table 7, the curve of UTR with $\Delta T = 50 \text{ K}$ coincides with that of LTR with $\Delta T = 100 \text{ K}$.

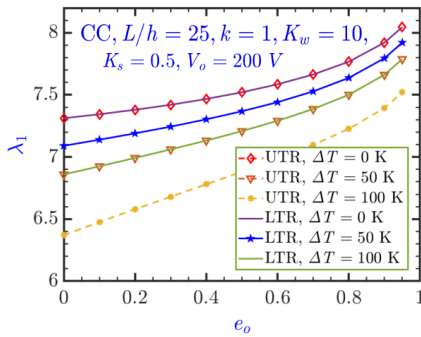


Figure 2. Effects of e_o and temperature rise on the frequency λ_1

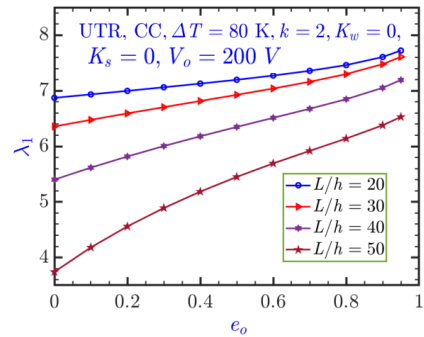


Figure 3. Effects of e_o and span-to-height ratio on the frequency λ_1

Variation of the non-dimensional frequency λ_1 with respect to e_o is portrayed in Fig. 3 for different values of span-to-height ratio L/h . The figure shows that the smaller L/h is, the greater λ_1 is obtained. This is due to the fact that the smaller L/h is, the greater the geometric stiffness of the beam is, since the slenderness of the beam decreases with the decreasing of L/h . Besides, the smaller L/h is, the smaller the rate of the increase in λ_1 with respect to e_o is.

Fig. 4 has the purpose to investigate the effect of temperature change ΔT and porosity coefficient e_o on the non-dimensional frequency λ_1 . As expected, the larger e_o is, the greater the frequency is obtained. It can be seen that the temperature change results in a reduction of the frequency. This is because an increase in the temperature change makes the compressive force N^{th} increase. Consequently, the stiffness of the system is reduced. The frequency vanishes as the temperature reaches the critical temperature. Furthermore, the rate of the reduction increases rapidly with increasing ΔT .

To examine the effects of boundary conditions (BCs) on the non-dimensional frequency λ_1 of the beam, Fig. 5 illustrates the variation of λ_1 with respect to ΔT for three cases of BC, i.e., SS, CH, and

CC. The figure shows that among the three BCs, the greatest and the smallest frequency λ_1 belong to CC and SS, respectively. Besides, the temperature that corresponds to the zero frequency of the CC beam is much higher when compared to that of the CH or SS one.

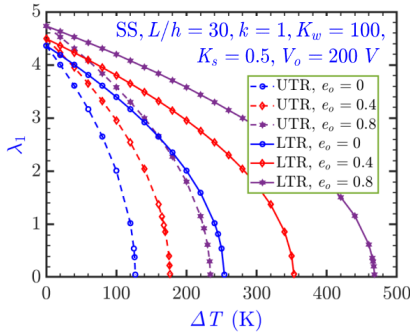


Figure 4. Variation of the frequency λ_1 with respect to ΔT

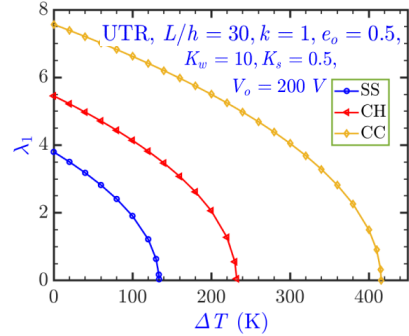
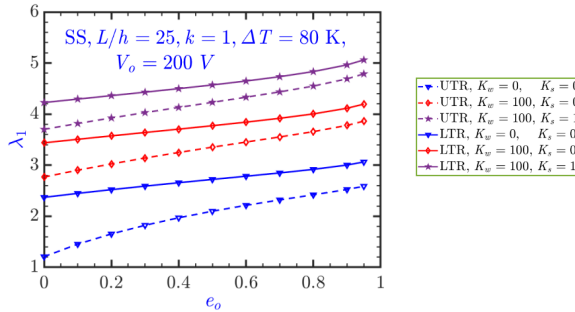
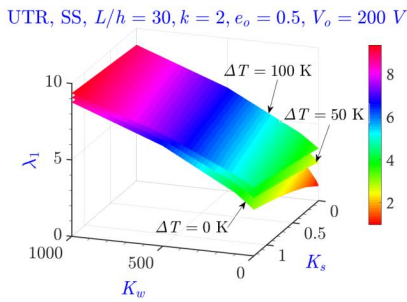


Figure 5. Effects of BCs and temperature change on the frequency λ_1

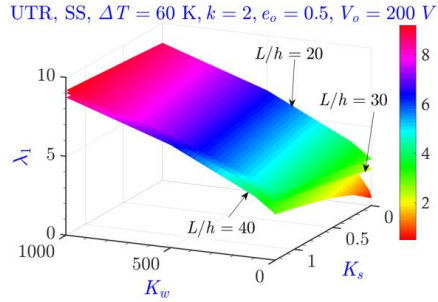
Finally, effects of elastic foundation coupled with porosity coefficient e_o /temperature change ΔT /span-to-height ratio L/h are plotted in Fig. 6. Observing the figures points out that the elastic foundation coefficients have strong effects on the frequency. These coupling effects are sensitive when the foundation coefficients are small.



(a) Coupling elastic foundation with e_o



(b) Coupling elastic foundation with ΔT



(c) Coupling elastic foundation with L/h

Figure 6. Effects of elastic foundation on the frequency λ_1

4. Conclusions

Thermo-electrical free vibration of FG sandwich beam composed of a metal foam core integrated with piezoelectric layers is investigated. The beam interacts with Pasternak foundation and is pre-stressed through a constant voltage and a uniform/linear temperature rise. Material properties of the core and two middle layers vary smoothly through the thickness direction. Lagrange equations in conjunction with the Reddy third-order beam theory are employed to derive the equilibrium equations of the system. The polynomial trial function-based Ritz method is adopted to obtain the approximate natural frequency. The correctness of the established theories is confirmed through comparative studies. Influences of geometry parameters, material property distribution, applied voltage, elastic foundation, temperature rises, i.e., UTR and LTR, temperature change, porosity coefficient, span-to-height ratio, and boundary conditions are investigated through parametric studies. From the numerical investigations, some important conclusions can be reached:

- Porosities have high effectiveness in enhancing the thermal vibration frequency of porous sandwich beams.
- The pre-stress caused by thermal loading has strong effects on the frequency of the beam; however, that by electrical one has insignificant effects.
- As the temperature change increases, the frequency is reduced and finally vanished at the critical temperature.
- The response of the symmetric layer structure beams under LTR with temperature change ΔT could be predicted through UTR with half of ΔT ($\Delta T/2$). This has a special meaning in practical implementation for simplifying the problem in analysis.
- Elastic foundation, power-law index, span-to-height ratio, and boundary supports also have important effects on the frequency.

References

- [1] Chen, D., Kitipornchai, S., Yang, J. (2016). [Nonlinear free vibration of shear deformable sandwich beam with a functionally graded porous core](#). *Thin-Walled Structures*, 107:39–48.
- [2] Wang, Y. Q., Zhao, H. L. (2019). [Free vibration analysis of metal foam core sandwich beams on elastic foundation using Chebyshev collocation method](#). *Archive of Applied Mechanics*, 89(11):2335–2349.
- [3] Grygorowicz, M., Magnucki, K., Malinowski, M. (2015). [Elastic buckling of a sandwich beam with variable mechanical properties of the core](#). *Thin-Walled Structures*, 87:127–132.
- [4] Srikarun, B., Songsuwan, W., Wattanasakulpong, N. (2021). [Linear and nonlinear static bending of sandwich beams with functionally graded porous core under different distributed loads](#). *Composite Structures*, 276:114538.
- [5] Wang, Y., Zhou, A., Fu, T., Zhang, W. (2019). [Transient response of a sandwich beam with functionally graded porous core traversed by a non-uniformly distributed moving mass](#). *International Journal of Mechanics and Materials in Design*, 16(3):519–540.
- [6] Hung, D. X., Truong, H. Q. (2018). [Free vibration analysis of sandwich beams with FG porous core and FGM faces resting on Winkler elastic foundation by various shear deformation theories](#). *Journal of Science and Technology in Civil Engineering (STCE) - NUCE*, 12(3):23–33.
- [7] Chinh, T. H., Tu, T. M., Duc, D. M., Hung, T. Q. (2020). [Static flexural analysis of sandwich beam with functionally graded face sheets and porous core via point interpolation meshfree method based on polynomial basic function](#). *Archive of Applied Mechanics*, 91(3):933–947.
- [8] Mu, L., Zhao, G. (2016). [Fundamental Frequency Analysis of Sandwich Beams with Functionally Graded Face and Metallic Foam Core](#). *Shock and Vibration*, 2016:1–10.

- [9] Derikvand, M., Farhatnia, F., Hodges, D. H. (2021). [Functionally graded thick sandwich beams with porous core: Buckling analysis via differential transform method](#). *Mechanics Based Design of Structures and Machines*, 1–28.
- [10] Kiani, Y., Rezaei, M., Taheri, S., Eslami, M. R. (2011). [Thermo-electrical buckling of piezoelectric functionally graded material Timoshenko beams](#). *International Journal of Mechanics and Materials in Design*, 7(3):185–197.
- [11] Kargani, A., Kiani, Y., Eslami, M. R. (2013). [Exact Solution for Nonlinear Stability of Piezoelectric FGM Timoshenko Beams Under Thermo-Electrical Loads](#). *Journal of Thermal Stresses*, 36(10):1056–1076.
- [12] She, G.-L., Shu, X., Ren, Y.-R. (2016). [Thermal buckling and postbuckling analysis of piezoelectric FGM beams based on high-order shear deformation theory](#). *Journal of Thermal Stresses*, 40(6):783–797.
- [13] Fu, Y., Wang, J., Mao, Y. (2012). [Nonlinear analysis of buckling, free vibration and dynamic stability for the piezoelectric functionally graded beams in thermal environment](#). *Applied Mathematical Modelling*, 36(9):4324–4340.
- [14] Khiem, N. T., Hai, T. T., Huong, L. Q. (2020). [Effect of piezoelectric patch on natural frequencies of Timoshenko beam made of functionally graded material](#). *Materials Research Express*, 7(5):055704.
- [15] Jankowski, P., Żur, K. K., Kim, J., Lim, C. W., Reddy, J. N. (2021). [On the piezoelectric effect on stability of symmetric FGM porous nanobeams](#). *Composite Structures*, 267:113880.
- [16] Singh, A., Kumari, P. (2020). [Two-Dimensional Free Vibration Analysis of Axially Functionally Graded Beams Integrated with Piezoelectric Layers: An Piezoelasticity Approach](#). *International Journal of Applied Mechanics*, 12(04):2050037.
- [17] Karamanlı, A. (2018). [Free vibration analysis of two directional functionally graded beams using a third order shear deformation theory](#). *Composite Structures*, 189:127–136.
- [18] Trinh, L. C., Vo, T. P., Thai, H.-T., Nguyen, T.-K. (2016). [An analytical method for the vibration and buckling of functionally graded beams under mechanical and thermal loads](#). *Composites Part B: Engineering*, 100:152–163.
- [19] Reddy, J. N. (2003). *Mechanics of Laminated Composite Plates and Shells*. CRC Press.
- [20] Aydogdu, M. (2006). [Free Vibration Analysis of Angle-ply Laminated Beams with General Boundary Conditions](#). *Journal of Reinforced Plastics and Composites*, 25(15):1571–1583.
- [21] Şimşek, M. (2010). [Fundamental frequency analysis of functionally graded beams by using different higher-order beam theories](#). *Nuclear Engineering and Design*, 240(4):697–705.
- [22] Mantari, J., Canales, F. (2016). [Free vibration and buckling of laminated beams via hybrid Ritz solution for various penalized boundary conditions](#). *Composite Structures*, 152:306–315.
- [23] Şimşek, M. (2015). [Bi-directional functionally graded materials \(BDFGMs\) for free and forced vibration of Timoshenko beams with various boundary conditions](#). *Composite Structures*, 133:968–978.
- [24] Pradhan, K., Chakraverty, S. (2013). [Free vibration of Euler and Timoshenko functionally graded beams by Rayleigh–Ritz method](#). *Composites Part B: Engineering*, 51:175–184.
- [25] Zahedinejad, P. (2016). [Free Vibration Analysis of Functionally Graded Beams Resting on Elastic Foundation in Thermal Environment](#). *International Journal of Structural Stability and Dynamics*, 16(07): 1550029.
- [26] Vo, T. P., Thai, H.-T., Nguyen, T.-K., Maheri, A., Lee, J. (2014). [Finite element model for vibration and buckling of functionally graded sandwich beams based on a refined shear deformation theory](#). *Engineering Structures*, 64:12–22.
- [27] Noori, A. R., Aslan, T. A., Temel, B. (2021). [Dynamic Analysis of Functionally Graded Porous Beams Using Complementary Functions Method in the Laplace Domain](#). *Composite Structures*, 256:113094.
- [28] Nguyen, T.-K., Nguyen, B.-D., Vo, T. P., Thai, H.-T. (2017). [Hygro-thermal effects on vibration and thermal buckling behaviours of functionally graded beams](#). *Composite Structures*, 176:1050–1060.